Electronic Supplementary Material (ESI) for ChemComm.

Probing Extracellular Acidity of Live Cells in Real Time for Cancer Detection and Monitoring Anti-Cancer Drug Activity

*Bhawana Thakur, S. Jayakumar and Shilpa N. Sawant**

Electronic Supplementary Information

1 Introduction

1(a) Techniques for measurement of tumor pH

Several techniques have been proposed for the measurement of tumor pH such as (a) positron emission tomography (PET), (b) Magnetic resonance spectroscopy/ imaging, (c) optical imaging using fluorescent dyes or fluorophore tagged proteins and (d) microelectrode measurements.

Magnetic resonance spectroscopy/ imaging utilizes the pH sensitive magnetic resonance of ^{31}P, ^{19}F or ^{1}H nuclei which are either inherently present in the tissue or added exogenously [1]. ^{31}P resonance studies using exogenous agent 3-aminopropylphosphate have confirmed that the average pH_e of tumors is acidic, with values reaching as low as 6.0 [2]. However, these techniques cannot be readily translated to the clinical settings [3].

PET involves use of radiolabeled compounds which distribute across the semipermiable membrane according to the pH gradient. This technique is the first noninvasive in vivo pH measurement technique and has been used since the last few decades [4]. pH (low) insertion peptide (pHLIP) are used to selectively accumulate in and label acidic tissues. Using pHLIP tagged radiotracer, Vavere *et al.* have measured the acidic environment in prostrate tumor [3].

Fluorescence-based techniques are widely used in biology for both imaging and sensing applications [5, 6]. They are mostly used for intracellular measurements, where typically pH sensitive dyes, or a combination of dyes are used to study the pH of intracellular organelles [5, 7]. Although the fluorescence based measurements provide a good estimation, they have drawback in terms of signal level, toxicity of the dyes and the complexity involved in tagging of fluorophore to the carrier proteins.

There are extensive reports in literature on measurement of pH of tumor tissues using pH electrodes. Wike-Hooley *et al.* [8] have presented a comprehensive review on pH values obtained in human tumor samples by microelectrode measurements. These measurements reveal that the pH values in human tumors are on an average lower than that observed in normal subcutaneous and muscle tissue. However, there is a large variation in the values reported by different groups, probably due to the undefined technical variables associated with pH measurements in tissues using electrodes [9]. The differences in the physiological and metabolic status of the patient at the time of analysis can also affect the results.

During most of the measurement, microelectrodes, typically ~ 1μm to a few mm size, are inserted in the tissue. This can lead to rupture of capillaries and can also damage the surrounding cells. Thus the measured pH value has a contribution from the pH of the extracellular fluid as well as an unknown contribution from damaged cells and blood released from ruptured capillaries [10]. This is a critical issue which needs to be addressed as the measured value is not specific to extracellular pH.

2. Experimental methods

A. Materials

Aniline (E. Merck) was distilled under reduced pressure and stored in dark. All aqueous solutions were prepared using deionized water with a resistivity greater than 18Mohm-cm from a Millipore Milli-Q system. Trypsin-EDTA, antibiotics (streptomycin and penicillin), Histopaque-1077, sodium chloride, potassium chloride, sodium dihydrogen phosphate, and potassium phosphate monobasic were purchased from Sigma-Aldrich (MO, USA). Dulbecco's Modified Eagles Medium (DMEM) and fetal bovine serum (FBS) were purchased from Himedia (Mumbai, India).

B. Cells culture and drug treatment

PC3 and DU145 prostate cancer cell lines were obtained from National Institute for Research in Reproductive Health, Mumbai, India. MCF7 cancer cells (mammary carcinoma cell line) and Chinese hamster ovarian (CHO) normal cells were obtained from National Centre for Cellular Sciences, Pune, India. Cells were maintained as exponentially growing monolayer in DMEM supplemented with 10% FBS, penicillin and streptomycin in humidified incubator maintained at 37^{o} C with 5% CO_2 in air. For pH measurement, exponentially growing cells were seeded overnight in culture dish, harvested by trypsinization, resuspended in 1xPBS (137 mM NaCl, 2.7 mM KCl, 10mM Na_2HPO_4, 2 mM KH_2PO_4 , pH 7.4) and then counted before the electrochemical measurement.

Peripheral blood mononucleated cells (PBMC) from human blood was isolated using Histopaque 1077 (Sigma, USA), as per the manufacturer's instructions. Briefly, 3 mL of peripheral blood was collected in a heparinised tube from healthy volunteers including the authors, layered on to 3mL of histopaque 1077 solution and centrifuged at 400 x g for 30 min at room temperature. After centrifugation, the buffy coat containing PBMC was removed carefully, washed with 10 mL 1x PBS two times, resuspended in PBS, counted and used for the experiment.

For the drug treatment studies, exponentially growing cells were seeded for overnight in the culture dish and then treated with respective drugs [either 100 µM Dexamethasone (Dex) or 100 µM 2-deoxy glucose (2DG)] for 24 hours before harvesting and followed by electrochemical measurement.

For imaging the uptake of 2DG by the cancer cells, MCF 7 cells were grown on a glass cover slip. The cells were incubated with 100 µl of glucose free culture medium having 150 µg/mL 2-[N-(7- nitrobenz-2-oxa-1, 3-diaxol-4-yl) amino]-2-deoxyglucose (2-NBDG)**.** After 10 min, the cover slip was washed with PBS (pH=7.4) to remove excess 2-NBDG. The cells were then immediately analysed using fluorescence microscope (excitation/ emission= 485/ 535 nm).

C. Sensor design and measurement

C1: Electrochemical cell set up

Electrochemical measurements were performed using an Autolab Potentiostat-Galvanostat, PGSTAT 20 (Eco Chemie, The Netherlands). Polyaniline deposition was carried out using a three electrode electrochemical cell with Ag/AgCl, KCl (3M) reference electrode and platinum wire auxiliary electrode. For sensor ***1***, gold inter-digitated electrode (electrode spacing 200 µm; finger width 500 µm) deposited on flexible plastic substrate was used as the working electrode (**Figure S2a**). For the sensor ***2***, gold electrodes with spacing of 25 µm (2 mm width) deposited on plastic substrate was used as the working electrode (**Figure S2b)**. For the sensing experiments, a two electrode assembly was fabricated to hold the electrolyte (50µl) and the cells.

C2: Polyaniline deposition

Polyaniline was deposited on the gold inter-digitated electrode by electropolymerisation using 0.1M aniline in 1 M hydrochloric acid solution. Potential of the working electrode was cycled between - 0.2 V to + 0.8 V (vs. Ag/AgCl reference electrode) at a scan rate of 50 mV/sec [11]. The deposition was carried out in 15 continuous scans to obtain a uniform film of polyaniline. For sensor electrode ***2***, polyaniline was deposited by placing a (5µL) droplet of the monomer solution over the 25µm electrode spacing followed by electropolymersation of the monomer using a three electrode assembly. The polymerisation was carried out in ten scans so as to bridge the gap between the electrodes with polyaniline.

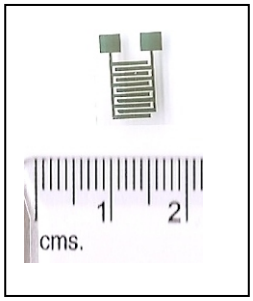

Figure S1 (a)

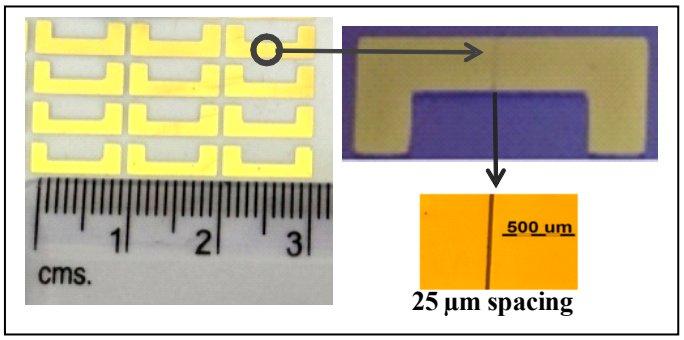

Figure S1 (b)

Figure S1a: Gold interdigitated electrode pattern (with finger spacing of 200µm) on flexible plastic substrate (electrode used in sensor ***1***).

Figure S1b: Gold electrodes with 25 µm spacing deposited on flexible plastic substrate (electrode used in sensor ***2***)

C3:Sensor response measurement

The measurement conditions (applied voltage, pulse time etc) were optimized to obtain maximum and stable response. Response of the sensor under optimized conditions was measured by applying a pulse of 0.4 V across the two terminals of the IDE for 5 seconds and the current obtained after 0.2 seconds was measured.

The normalized current (I) was calculated as
$I = (I_t - I_0) / I_0$,
where I_t = current measured on addition of cells, I_0= current measured in the absence of cells. Normalization of the current took care of the variation in current values obtained for different sensor films due to change in electrode area and other geometric parameters. All the experiments were repeated three to six times and the results obtained were reproducible.

C4: Sensor calibration

Each sensor film was first calibrated for pH measurements using PBS solutions of different pH ranging from 5 to 8 (Figure 2). The normalized current was calculated using the current at pH = 8 as the I_0 value. The normalized current values enable direct read-out of pH values using the calibration curve.

C5: Sensor response to cancer cells

In a typical sensing experiment, the sensor electrode was equilibrated with PBS (pH = 8) till a stable background current was reached. Aliquots of the cell suspension were added to 50 μL of PBS (pH = 8) solution which was used as the electrolyte in the sensor assembly (Fig. S2b). The amperometric current response was measured at different time intervals on addition of the cells to the electrolyte. It was observed that the current response initially increased rapidly with time and almost saturated after a time interval of ~ 20 minutes, hence this waiting time was used for further measurements. This delay could be the time required for the cells to settle down and directly interact with the sensor surface.

From the amperometric response, the normalised current was calculated (section C3) and using the sensor calibration curve, the corresponding pH value was obtained.

C6: Measuring Glycolysis inhibtion on drug treatment

The MCF7 cells were treated with 100 μM drug Dexamethasone (Dex) or 2-deoxy glucose (2DG) for 24 hours. The drug treated cells were harvested, washed with PBS, counted and suspended in PBS solution of pH=8. These washed cells were placed over the sensor surface and the response was monitored at different cell density as well as over a period of time. After 30 minutes, 5mM glucose was added to the electrolyte in the sensor assembly and the response of the cells was monitered over a period of time. The inhibition efficiency was calculated based on the sensor response of the control MCF7 cells (not treated with drug) and the sensor response of the drug treated cells.

3. Results & Discussion

3A. Amperometric response of sensor 1

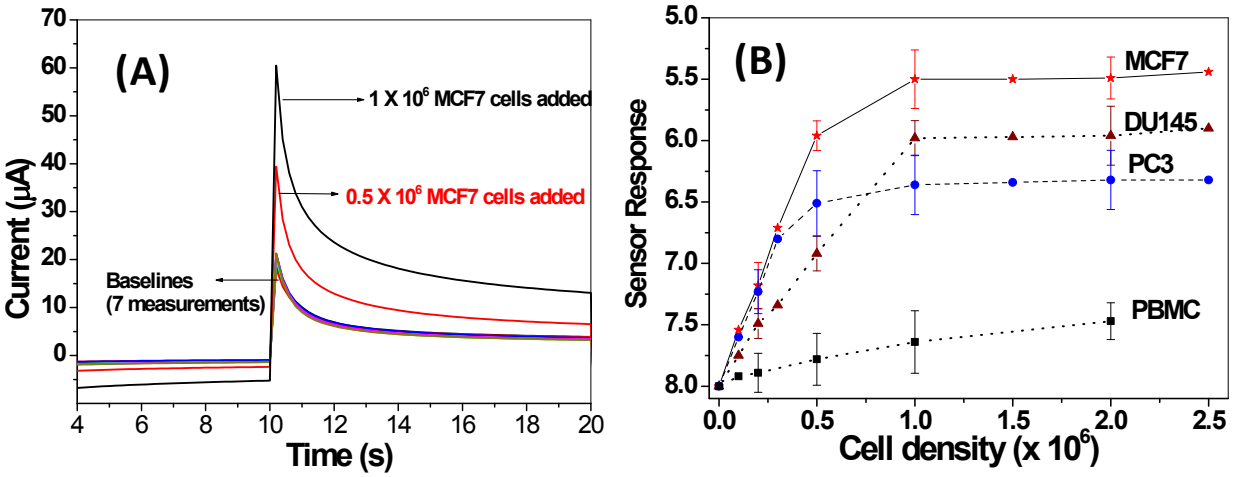

Figure S2: **(A)** Amperometric response of the sensor ***1*** on addition of MCF7 cells. Baseline shows variation in seven blank values recorded (in the absence of MCF7 cells) over a span of 30 mins. **(B)** Response of the sensor ***1*** to different densities of (a) PC3, (b) MCF7, (c) DU 145, and (d) Normal PBM cells. Error bars correspond to N=5.

(Response of the sensor in Figure S2(B) corresponds to the pH values calculated from the normalised current and the calibration curve as described in Section 2*C3* and 2*C5* on page 5)

3B. Optical and Fluorescence microscopy studies

Optical & Fluorescence microscopy studies were carried out using Olympus BXS3 (Japan) microscope in reflectance mode. FITC was used for cell staining in fluorescence microscopy studies.

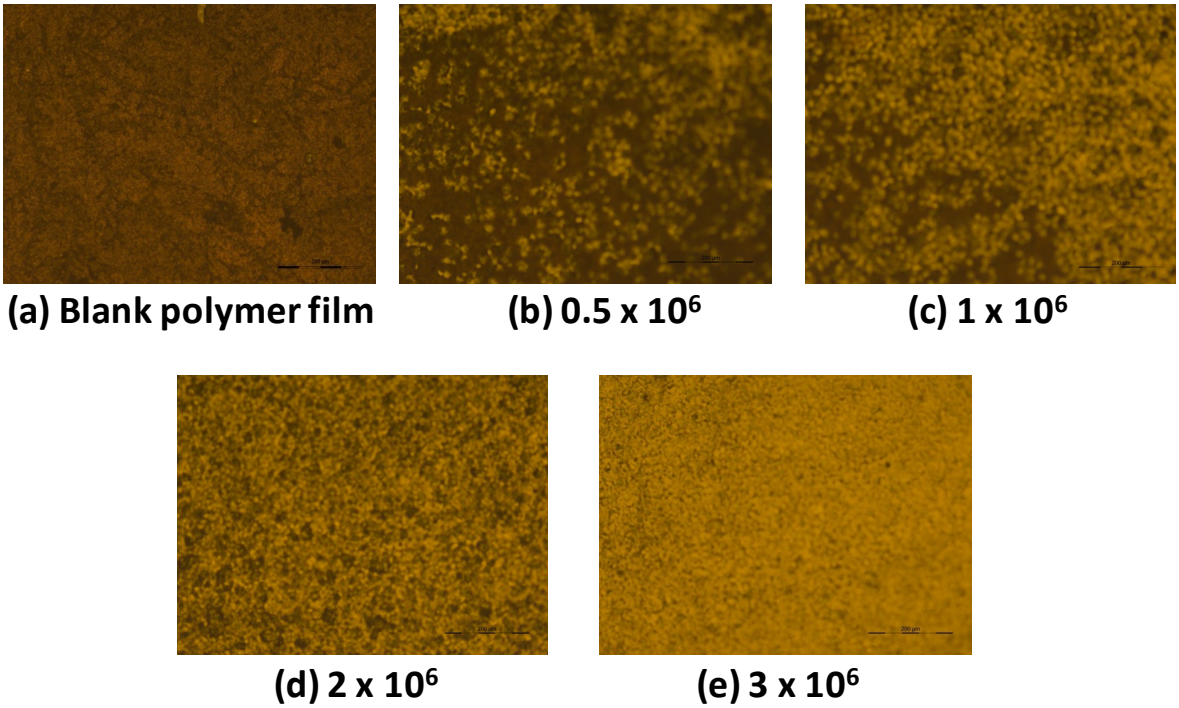

Figure S3*: Optical microscopy images of (a) blank polyaniline sensor film, sensor film with (b) 0.5 x 10^6, (c) 1 x 10^6, (d) 2 x 10^6 and (e) 3 x 10^6 PC3 cells immobilized on sensor active area. Bar= 200 µm*

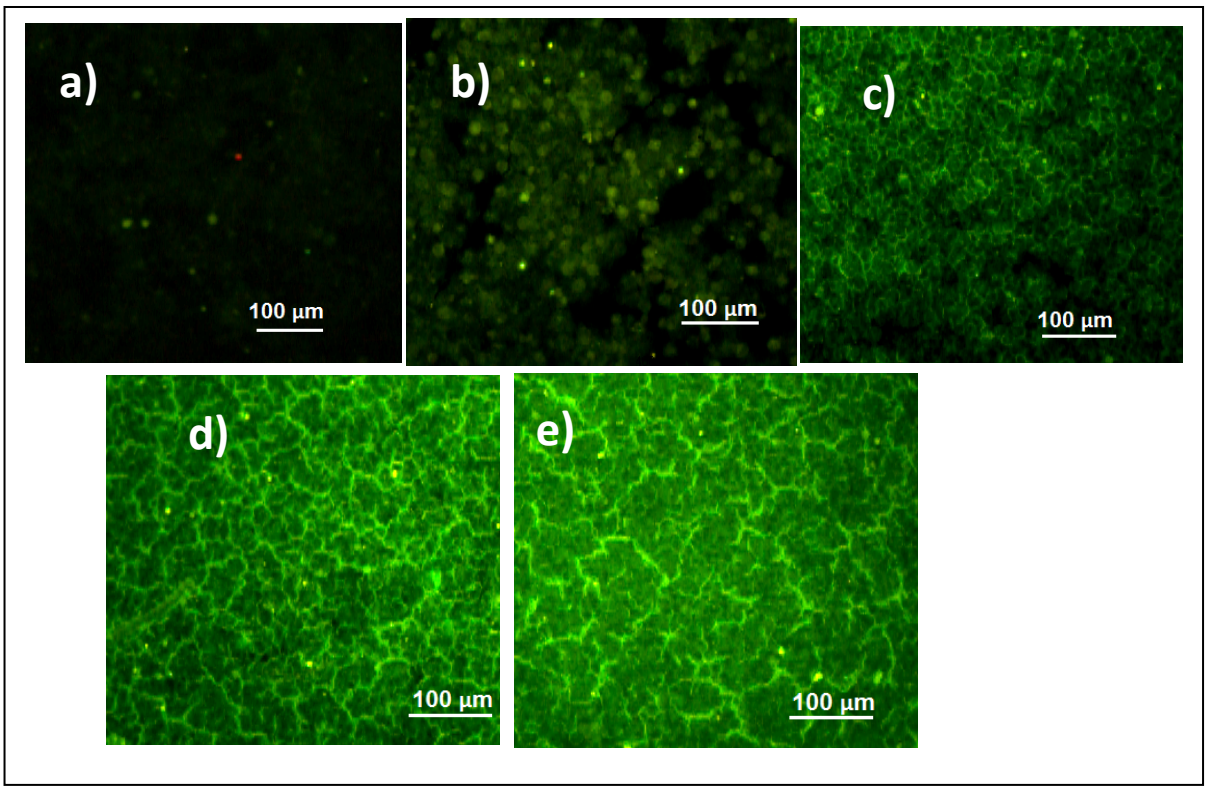

Figure S4*: Fluorescence microscopy images of sensor film with (a) 0.1× 10⁶ cells, (b) 0.5× 10⁶ cells, (c) 1× 10⁶ cells, (d) 1.5× 10⁶ cells and (e) 2× 10⁶ MCF7 cells. Bar = 100 µm*

3C. ***Zeta potential measurements***

To elucidate the nature of extracellular environment and its probable correlation with pH_e, we have also carried out Zeta potential measurement of the cells suspended in PBS (pH= 7.4). Zeta potential is the electrostatic potential at the shear plane of the charged particle and thus is related to the surface charge and the local environment. Zeta potential of all the cells studied was found to be negative with the highest value for PCMB cells followed by MCF7 (N= 5). However, no direct correlation or trend was observed between the zeta potential and the pH_e values recorded for the different cell types studied. The charge of the cell membrane is predominantly determined, among other factors, by the type of glycoproteins and phospholipid head groups present in the membrane [12]. The acidic metabolites released by the cells do not seem to contribute significantly to the zeta potential values, thus no correlation with pH_e was observed

Sr. No.	Cell type	Zeta potential (mV)	pH_e
1	MCF7	-12.59 ± 0.91	5.49
2	DU145	-9.58 ± 0.70	5.96
3	PC3	-14.00 ± 0.51	6.34
4	PBMC	-13.87 ± 1.25	7.47

Table S1: Zeta potential and pH_e values for the different cells studied.

The zeta-potential measurements were carried out using Zetasizer nano series (from Malvern Instruments, UK) using disposable zeta-potential cells with gold-coated electrodes at 25 °C.

.

3D. ***Tumor pH values reported in literature***

Table S2: Extracellular (pH_e), Intracellular (pH_i) and tumor pH values reported in literature using different techniques.

Cell type	pHe	Technique	Ref (No.)	Year of publication
Positron Emission Tomography (PET)				
PC3	7.23±0.1 (N=3)	PET	3	2009
LNCaP	6.78±0.29			
Magnetic resonance spectroscopy (MRS)				
PC3	6.8±0.11 (N=7)	^{31}P-MRS	13	2012
Lymphoma xenograft	6.7±0.1	^{13}C MRS	4	2010
PC3- subcutaneous tumor	6.97	^{1}H MRS	14	2009
PC3-orthotopic tumor	6.62			
Human subcutaneous (normal)	7.63±0.034			
Normal tissue	7.2-7.5			
MDA-MB-231 (Adenocarcinoma)	7.0 ± 0.11	^{31}P MRS	15	2009
Normal tissue	7.4±0.08			
MCF7	6.6	^{31}P MRS	16	1999
RIF-1	6.80±0.04	^{31}P and ^{19}F MRS	17	1999
HT29	6.83±0.03			
H9618a	6.79±0.34			
GH3	7.15±0.03			
pH Electrode measurements				
P388 murine monocytic leukaemia tumours	6.3	pH microelectrode	18	2009
Normal tissues (DBA/2 mice)	7.3			

Human lung carcinoma54A	6.77±0.03	Glass microelectrode	19	2006
Human mammary carcinoma	7.29±0.05 (minimum value= 6.9)	Philips tissue pH electrode	20	2004
Human subcutis (normal)	7.63±0.034			
Tumor cells	Avg. 6.8-7.2	pH electrode	21	1996
Normal cells	Avg. 7.4			
Lung fibroblast(Chinese hamster)	Parental =6.65±0.07 Variant=6.78±0.04 (n=12)	Glass microelectrode	22	1993
Normal muscle cell	7.29±0.06 (n=12)			
30 human tumour xenograft Normoglycemia Temporary increase in plasma glucose	6.83 (range, 6.72-7.01; n = 268). 6.43 (range, 6.12-6.78; n = 292)	H+ ion-sensitive semi-microelectrode	23	1993
Normal tissue Normoglycemia Temporary increase in plasma glucose	7.14 6.97			
Lung cancer	6.79			
Gastrointestinal cancer	6.84			
Sarcomas	6.93			
Human mammary carcinoma	6.85			
Dysplasia	7.05±0.2	Miniature needle pH electrode	24	1988
Benign tumor	6.95±0.19			
Malignant tumor	6.94±0.19			
Yoshida sarcoma	6.87±-0.21			
Human tumors	5.55-7.69 (Avg 6.81±0.09)	21 gauge needle electrode	25	1985
Rat intestine/ jejunum	6.1	pH electrode	26	1983
Distal ileum	7.3			

Fluorescence measurements				
Lysosomes (Chinese Hamster Ovary cells)	5.2 ±0.7 (confocal microscope) 5.1±0.5 (fluorescence spectroscopy)	Fluorescence pH nanosensor	27	2012
Melanoma MV3 cell	7.46-6.73(outer buffer pH 7.2) 7.66-6.81(outer buffer pH 6.55)	Fluorescence (proton-sensitive dyes, fluorescein conjugates)	28	2007
Lysosomes (Human ML-IV cells)	5.24±0.35	Fluoresence	29	1999
Lysosomes (normal cells)	4.46±0.08			
MCF7 lysosomes	5.13±0.48 (*n*=14)	Video-enhanced epifluorescence	30	1994
MDA-MB231 lysosomes	5.06±0.7 (n=8)			
Large acidic vesicles	~ 4			

3E. ***Sensor characteristics***

Table S3. Sensor characteristics for detection of cancerous and non cancerous cells .

Sensor type	Cell type	Sensitivity (pH units per cell) [a]	Linear range (cell number)	R^2 [b]	Detection limit (cell density) [c]
1	MCF7	$(4.07 \pm 0.43) \times 10^{-6}$	0 - 0.5 x 10^6	0.9992	4.91 x 10^3
	PC3	$(3.97 \pm 0.079) \times 10^{-6}$	0 - 0.3 x 10^6	0.9996	5.04 x 10^3
	DU145	$(1.99 \pm 0.055) \times 10^{-6}$	0 - 1.0 x 10^6	0.9985	1.01 x 10^4
	PBMC	$(0.34 \pm 0.030) \times 10^{-6}$	0 - 1.0 x 10^6	0.9885	5.88 x 10^4
2	MCF7	$(3.1 \pm 0.37) \times 10^{-2}$	0 - 40	0.9856	2 (LOD value) 5 (LOQ value)

[a] Slope of linear region of the calibration curve; [b] Correlation coefficient of the linear range;
[c] Detection limit calculated based on sensitivity at pH values ~ 6.

LOD: Limit of detection; estimated at 3σ, σ = standard deviation of background signal.
LOQ: Limit of quantification; determined by measuring progressively more dilute solutions of analyte (cells)

3F. Cell viability studies

Live and dead assay performed in MCF7 cells after treating with drug (2DG or Dex) using trypan blue staining

Representative images of the microscopic field containing live and dead cells. Control and drug treated MCF7 cells were harvested after trypsinization, stained with trypan blue and visualized using an inverted microscope, and the number of live and dead cells were enumerated.

(a) 2DG treated MCF7 cells

Group	Total cells	Dead Cells	% of dead cells
Control	250	5	2%
2DG	283	10	3.5%

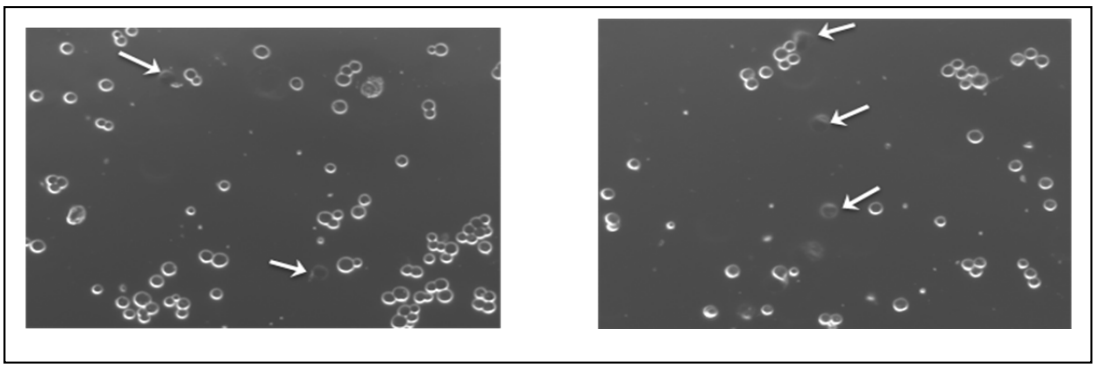

Control (at 20x magnification) 2DG

(b) Dex treated MCF7 cells

Group	Total cells	Dead Cells	% of dead cells
Control	200	3	1.5 %
Dexamethasone	200	3	1.5 %

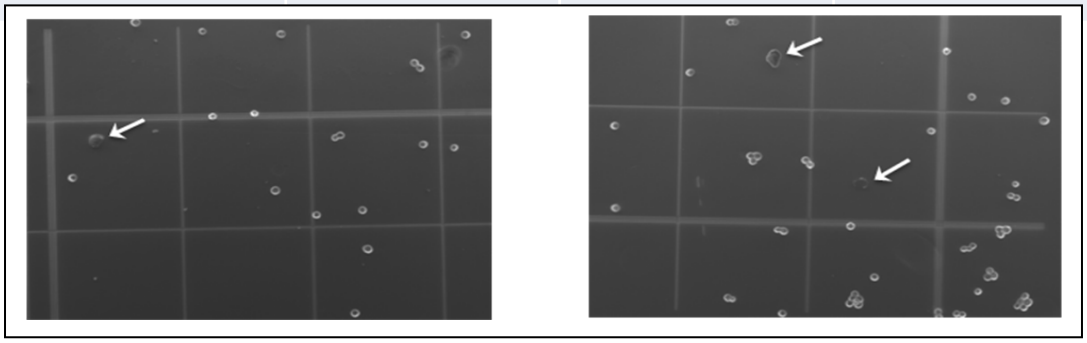

Control (at 10x magnification) Dexamethasone

4. References

1. R. J. Gillies, N. Raghunand, M. L. Garcia-Martin and R. A. Gatenby, *IEEE Eng. Med. Biol.,* 2004, **23**, 57-64.
2. R. J. Gillies, N. Raghunand, G. S. Karcamar and Z. M. J. Bhujwalla, *Magn. Reson. Imaging*, 2002, **16**, 430-450.
3. A. L. Vavere, G. B. Biddlecombe, W. M. Spees, J. R. Garbow, D. Wijesinghe, O. A. Andreev, D. M. Engelman, Y. K. Reshetnyak and J. S. Lewis, *Cancer Res*., 2009, **69**, 4510-4516.
4. X. Zhang, Y. Lin and R. J. Gillies, *J. Nucl. Med*., 2010, **51**, 1167-1170.
5. M. Verdoes, K. O. Bender, E. Segal, W. A. Linden, S. Syed, N. P. Withana, L. E. Sanman and M. Bogyo, *J. Am. Chem. Soc.,* 2013, **135,** 14726-14730.
6. A. Bajaj, O. R. Miranda, R. Phillips, I. B. Kim, D. J. Jerry, U. H. F. Bunz and V. M. Rotello, *J. Am. Chem. Soc.,* 2010, **132**, 1018-1022.
7. H. Zhang, J. Fan, J. Wang, S. Zhang, B. Dou and X. Peng, *J. Am. Chem. Soc.,* 2013, **135**, 11663-11669.
8. L. Wike-Hooley, J. Haveman and H. S. Reinhold, *Radiother. Oncol*., 1984, **2**, 343-366.
9. L. E. Gerweck, *Semin. Radiat. Oncol.* 1998, **8**, 176-182.
10. I. F. Tannock and D. Rotin, *Cancer Res*., 1989, **49**, 4373-4384.
11. M. U. A. Prathap, A. K. Chaurasia, S. N. Sawant and S. K. Apte, *Anal. Chem*., 2012, **84**, 6672-6678.
12. S. Ran, A. Downes, P. E. Thorpe, *Cancer Res.,* 2002, **62**, 6132-6140.
13. S. Macholl, M. S. Morrison, P. Iveson, B. E. Arbo, O. A. Andreev, Y. K. Reshetnyak, D. M. Engelman, E. Johannesen, *Mol. Imaging Biol*., 2012, **14,** 725-734.
14. M. F. Penet, A. P. Pathak, V. Raman, P. Ballesteros, D. Artemov, Z. M. Bhujwalla, *Cancer Res*., 2009, **69**, 8822-8829.
15. I. F. Robey, B. K. Baggett, N. D. Kirkpatrick, D. J. Roe, J. Dosescu, B. F. Sloane, A.I. Hashim, D. L. Morse, N. Raghunand, R. A. Gatenby, R. J. Gillies, *Cancer Res.,* 2009, **69**, 2260-2268.
16. N. Raghunand, M. I. Altbach, R. van Sluis, B. Baggett, C. W. Taylor, Z. M. Bhujwalla, R. J. Gillies, *Biochemical Pharmacology,* 1999, **57**, 309-312.
17. M. Stubbs, P. M. J. McSheehy, J. R. Griffiths, C. L. Bashford, *Mol. Med. Today*, 2000, **6**, 15-29.
18. D. Lindner, D.Raghavan, *Br. J. Cancer,* 2009, **100**, 1287-1291.
19. L. E. Gerweck, S. Vijayappa, S. Kozin, *Mol. Cancer Ther.,* 2006, **5**, 1275-1279.

20. A. P. Van Den Berg, J. L. Wike-Hooley, A. F. Van Den Berg-Block, J. Van Der Zee, H. S. Reinhold, *Eur. J. Cancer Clin. Oncol.,* 1982, **18,** 457-462.
21. L. E. Gerweck, K. Seetharaman, *Cancer Res.* 1996, ***56,*** 1194-1198.
22. K. Newell, A. Franchi, J. Pouyssegur, I., *Proc. Natl. Acad. Sci.,* 1993, **90**, 1127-1131.
23. T. Volk, E. Jaihde, H. P. Fortmeyer, K. H. Glisenkamp, M. F. Rajewsky, *Br. J. Cancer,* 1993, **68**, 492-500.
24. P. Vaupel, F. Kallinowaski, P. Okunieff, *Cancer Res.,* 1989, **49***,* 6449-6465.
25. A. J. Thistlethwaite, D. B. Leeper, D. J. Moylan and R. E. Nerlinger, *Int. J. Radiat. Oncol. Bio. Phys.,* 1985, **11**, 1647-1652.
26. M. Lucas, *Gut.,* 1983, **24**, 734-739.
27. M. J. Marin, F. Galindo, P. Thomas, D. A. Russell, *Angew. Chem. Int. Ed.,* 2012, **51,** 9657-96661.
28. C. Stock, M. Mueller, H. Kraehling, S. Mally, J. Noel, C. Eder, A.Schwab, *Cell Physiol. Biochem.,* 2007, **20**, 679-686.
29. G. Bach, C. S. Chen, R. E. Pagano, *Clin. Chim. Acta.* 1999, **280,** 173-179.
30. P. Montcourrier, P. H. Mangeat, C. Valembois, G. Salazar, A. Sahuquet, C. Duperray, H. Rochefort, *J.Cell Sci.,* 1994, **107,** 2381-2391.